Molecular Pharmacology Fast Forward. Published on July 26, 2018 as DOI: 10.1124/mol.118.111674
This article has not been copyedited and formatted. The final version may differ from this version.

RGS10 regulates the expression of Cyclooxygenase-2 and Tumor Necrosis Factor alpha through a G protein-independent mechanism[a]

Mohammed Alqinyah, Faris Almutairi, Menbere Y. Wendimu, Shelley B. Hooks.

Primary lab of Origin: Hooks lab, Department of Pharmaceutical and Biomedical Sciences, University of Georgia (M.A., F.A., M.Y.W., S.B.H.)

Molecular Pharmacology Fast Forward. Published on July 26, 2018 as DOI: 10.1124/mol.118.111674
This article has not been copyedited and formatted. The final version may differ from this version.

RGS10 regulates the expression of Cyclooxygenase-2 and Tumor Necrosis Factor alpha through a G protein-independent mechanism

Running title: RGS10 regulation of COX-2

Corresponding author:
Shelley B. Hooks
240 West Green Street
Pharmacy South
University of Georgia
Athens, GA 30602
Phone: 706-542-2189
Fax: 706-542-5358
Email: shooks@uga.edu

Text pages: 28

Tables: 0

Figures: 6

References: 48

Abstract words: 250

Introduction words: 507

Discussion words: 1548

Abbreviations: Cyclooxygenase (COX), G protein coupled receptor (GPCR), GTPase accelerating protein (GAP), lipopolysaccharide (LPS), Lysophosphatidic Acid (LPA), pertussis toxin (Ptx), Prostaglandin E2 (PGE2), Regulator of G protein Signaling (RGS), Toll-like receptor (TLR), Tumor necrosis factor (TNF).

Molecular Pharmacology Fast Forward. Published on July 26, 2018 as DOI: 10.1124/mol.118.111674
This article has not been copyedited and formatted. The final version may differ from this version.

Abstract.

The small RGS protein RGS10 is a key regulator of neuroinflammation and ovarian cancer cell survival; however, the mechanism for RGS10 function in these cells is unknown and has not been linked to specific G protein pathways. RGS10 is highly enriched in microglia, and loss of RGS10 expression in microglia amplifies production of the inflammatory cytokine TNFα and enhances microglia-induced neurotoxicity. RGS10 also regulates cell survival and chemoresistance of ovarian cancer cells. Cyclooxygenase-2 (COX-2) mediated production of prostaglandins such as PGE2 is a key factor in both neuroinflammation and cancer chemoresistance, suggesting it may be involved in RGS10 function in both cell types, but a connection between RGS10 and COX-2 has not been reported. To address these questions, we completed a mechanistic study to characterize RGS10 regulation of TNFα and COX-2 and to determine if these effects are mediated through a G protein dependent mechanism. Our data show for the first time that loss of RGS10 expression significantly elevates stimulated COX-2 expression and PGE2 production in microglia. Further, the elevated inflammatory signaling resulting from RGS10 loss was not affected by Gαi inhibition, and a RGS10 mutant that is unable to bind activated G proteins was as effective as wildtype in inhibiting TNFα expression. Similarly, suppression of RGS10 in ovarian cancer cells enhanced TNFα and COX-2 expression, and this effect did not require Gi activity. Together, our data strongly indicate that RGS10 inhibits COX-2 expression by a G protein independent mechanism to regulate inflammatory signaling in microglia and ovarian cancer cells.

Molecular Pharmacology Fast Forward. Published on July 26, 2018 as DOI: 10.1124/mol.118.111674
This article has not been copyedited and formatted. The final version may differ from this version.

1. Introduction.

Regulators of G protein signaling (RGS) are a family of proteins that classically act as activators of the intrinsic GTPase activity of heterotrimeric Gα subunits (Watson et al., 1996). Owing to this GTPase-accelerating protein (GAP) activity and inhibition of signaling initiated by G protein coupled receptors, RGS proteins play numerous roles in physiological and pathological conditions in diverse systems. However, multiple studies have revealed actions of RGS proteins that are independent of GTPase-accelerating activity, recently reviewed in: (Sethakorn et al., 2010). These non-canonical functions of RGS proteins can affect a variety of targets, including GPCRs, kinases, and transcription factors (Sethakorn et al., 2010). Therefore, to investigate the molecular mechanism of specific RGS protein actions, a critical initial question to answer is whether the RGS protein is acting in a classic GAP-dependent or non-canonical GAP-independent mechanism. The small RGS protein RGS10 regulates inflammatory and survival signaling in multiple cell types (Hooks et al., 2010; Lee et al., 2013; Lee et al., 2011), and has been proposed as a potential drug target for neuroinflammatory disease and ovarian cancer. However, the mechanisms by which RGS10 affects inflammatory and survival signaling are undefined, hampering the development of RGS10-targeted therapeutic strategies.

RGS10 is the smallest member of the R12 RGS subfamily with no functional domains outside of the RGS domain. RGS10 has been shown to selectively target Gαi family G proteins via classic GAP activity (Hunt et al., 1996), and is highly enriched in immune cells, including peripheral macrophages and microglia (Lee et al., 2013; Lee et al., 2008). Loss of RGS10 in microglia amplifies production of inflammatory cytokines, such

Molecular Pharmacology Fast Forward. Published on July 26, 2018 as DOI: 10.1124/mol.118.111674
This article has not been copyedited and formatted. The final version may differ from this version.

as TNFα and interleukin 1β, and enhances microglia-induced neurotoxicity triggered by the toll-like receptor ligand lipopolysaccharide (LPS) (Lee et al., 2011). Reciprocally, activation of microglia by LPS induces epigenetic silencing of RGS10, which we predict serves to amplify inflammatory signaling (Alqinyah et al., 2017). In addition to its anti-inflammatory role in microglia, RGS10 also regulates survival of ovarian cancer cells, and loss of RGS10 induces chemoresistance in ovarian cancer cells (Ali et al., 2013; Hooks et al., 2010). Cyclooxygenase-2 (COX-2) mediated production of prostaglandins such as PGE2 is also a key factor in both neuroinflammation and cancer chemoresistance (Bijman et al., 2008; Minghetti, 2004), suggesting that this pathway may be related to RGS10 effects, but the effect of RGS10 on COX-2 expression and function is not known.

The goal of the current study was to test the hypothesis that RGS10 regulates TNFα and COX-2 through a GAP-dependent mechanism. Our data show for the first time that RGS10 deficiency significantly elevates LPS-stimulated COX-2 expression and release of PGE2 from microglia. Furthermore, the elevated inflammatory signaling resulting from RGS10 loss was not affected by Gαi inhibition, and a RGS10 GAP-deficient mutant was as effective in inhibiting TNFα expression as wild type RGS10, suggesting that the anti-inflammatory functions of RGS10 are not mediated by its classic GAP activity on G proteins. We also show for the first time that RGS10 regulates TNFα and COX-2 expression in ovarian cancer cells through a Gi-independent mechanism.

2. Materials and Methods.

2.1. Cells and Reagents.

Molecular Pharmacology Fast Forward. Published on July 26, 2018 as DOI: 10.1124/mol.118.111674
This article has not been copyedited and formatted. The final version may differ from this version.

Murine BV-2 microglia cell line was a gift from G. Hasko at University of Medicine and Dentistry of New Jersey (Newark, NJ) and was previously generated by Blasi E et al. (Blasi et al., 1990). BV-2 cells were maintained in Dulbecco's Modified Eagle's Medium (DMEM) (VWR) supplemented with 10% Fetal Bovine Serum (ThermoFisher Scientific). The HEK-Blue™ hTLR4 cell line was purchased from Invivogen and was maintained in Dulbecco's Modified Eagle's Medium (DMEM) (VWR) with 10% Fetal bovine serum and HEK-Blue™ Selection antibiotics (Invivogen) to selectively maintain cells over-expressing TLR4 and adapter proteins. The human SKOV-3 cell line was purchased from ATCC and was maintained in McCoy's 5A, 1X (Iwakata & Grace Mod.) medium (Corning) supplemented with L-glutamine and 10% FBS.

Lipopolysaccharide was purchased from Sigma-Aldrich (St. Louis, MO), recombinant mouse CXCL12/SDF-1 alpha protein was purchased from R&D systems (Minneapolis, MN), Pertussis Toxin was obtained from Tocris (Pittsburgh, PA) and lysophosphatidic acid (LPA) was from Avanti Polar Lipids (Alabaster, AL).

2.2 siRNA and plasmid transfection

Mouse and human siRNA duplexes were purchased from Santa Cruz Biotechnology (mouse: sc-36411, human: sc-36410) and Lipofectamine-LTX with PLUS reagent was purchased from Thermo Fisher Scientific. The mouse siRNA used herein is the same as was described and validated by Lee et al (Lee et al., 2008). The final concentration of siRNA in the culture medium was 60 nM, and the transfection was performed according to the manufacturer's protocol. Following transfection, cells were cultured an additional 48 hours in an antibiotic free culture medium before assessing expression or function. The specificity of knock down was determined by comparing expression of RGS10 with

Molecular Pharmacology Fast Forward. Published on July 26, 2018 as DOI: 10.1124/mol.118.111674
This article has not been copyedited and formatted. The final version may differ from this version.

RGS2, which is also highly expressed in microglia, and RGS12 and RGS14, which exhibit highest sequence similarity to RGS10 (Supplementary data Figure 1). RT-PCR was performed using primer sequences: Mouse RGS10 Forward: 5'-TCCATGACGGAGATGGGAG-3', Mouse RGS10 Reverse: 5'-AACAAGACATTCTCTTCGCTGAA-3', Mouse RGS2 Forward: 5'-GAGAAAATGAAGCGGACACTCT-3', Mouse RGS2 Reverse: 5'-GCAGCCAGCCCATATTTACTG-3', Mouse RGS12 Forward: 5'-GTGACCGTTGATGCTTTCG-3', Mouse RGS12 Reverse: 5'-ATCGCATGTCCCACTATTCC-3', Mouse RGS14 Forward: 5'-AAATCCCCGCTGTACCAAG-3', Mouse RGS14 Reverse: 5'-GTGACTTCCCAGGCTTCAG-3'.

Ha-tagged RGS10-2 DNA plasmids were purchased from cDNA resource center (Bloomsburg University). The E52K mutation was generated with the QuikChange site directed mutagenesis kit (Stratagene) using primer sequences:(forward: 5'-TA AAA AAG GAA TTC AGT GAA **A**AA AAT; reverse: 5'-GC TAG CCA AAA CAA AAC ATT TT**T** TTC A). Mutagenesis resulted in a single nucleotide change from G→A, corresponding to codon GAA→AAA, Glutamic acid→ lysine at position 52 of human RGS10-2.

For transfection, 0.5 μg of plasmid DNA was used per well of a 24 well plate, or scaled up or down appropriately for different size wells or plates. DNA plasmids were added to cells with Lipofectamine reagent according to the manufacturer's instructions, and cells were cultured an additional 48 hours in antibiotic free medium prior to assessing function.

Molecular Pharmacology Fast Forward. Published on July 26, 2018 as DOI: 10.1124/mol.118.111674
This article has not been copyedited and formatted. The final version may differ from this version.

2.3. Western Blot Analysis.

Cells were lysed in SDS-PAGE sample buffer (0.5 M Tris pH 6.8, 10% SDS, Glycerol, β-mercaptoethanol, bromophenol blue) and samples were subjected to SDS-PAGE using standard protocols followed by transfer to nitrocellulose membranes. Primary antibodies for RGS10, COX-2, P65, and GNAI3 were purchased from Santa Cruz Biotechnology (Dallas, TX). P-ERK, ERK, P-P65, P-AKT, AKT were obtained from Cell Signaling Technology (Danvers, MA), and GAPDH was purchased from Millipore Technologies (Temecula, CA). Following primary antibody incubation, the suitable secondary HRP-conjugated antibodies were used to incubate the membranes: donkey anti-goat IgG-HRP (Santa Cruz), Goat Anti-Rabbit IgG-HRP (Millipore), and Goat anti-Mouse IgG-HRP (Bethyl). The membranes were visualized utilizing an enhanced chemiluminescent substrate for detection of HRP (ThermoScientific), and quantified using Flourchem HD2 software. The values were normalized to endogenous control GAPDH.

2.4. Quantitative Real-Time Polymerase Chain Reaction.

Isolation of mRNA was performed using TRIzol reagent (Invitrogen/Life Technologies, Carlsbad, CA) and cDNA was synthesized using High-Capacity cDNA Reverse Transcription Kit (Applied Biosystems). Actin and/or glyceraldehyde-3-phosphate dehydrogenase (GAPDH) were used as housekeeping genes for normalization. Calculating the fold difference was performed using the $2^{-\Delta\Delta CT}$ method. Mouse actin and COX-2 mouse and human primers were purchased from Sigma. Mouse TNFα primers and human GAPDH and TNFα primers were obtained from Integrated DNA

Molecular Pharmacology Fast Forward. Published on July 26, 2018 as DOI: 10.1124/mol.118.111674
This article has not been copyedited and formatted. The final version may differ from this version.

Technologies, IDT. Mouse primers used: actin forward 5′-GGC TGT ATT CCC CTC CAT CG-3′, actin reverse 5′-CCA GTT GGT AAC AAT GCC ATG T-3′, Cox-2 forward 5'-TGCAAGATCCACAGCCTACC-3', Cox-2 reverse 5'- GCTCAGTTGAACGCCTTTTG-3', TNF-α forward, 5′-CCT GTA GCC CAC GTC GTA G-3′; TNF-α reverse, 5′-GGG AGT AGA CAA GGT ACA ACC C-3′. Human primers used: GAPDH forward, 5′-GCCAAGGTCATCCATGACAACT-3', GAPDH reverse, 5′-GAGGGGCCATCCACAGTCTT-3', TNF-α forward, 5′-CTCTTCTGCCTGCACTTTG-3', TNF-α reverse, 5′-ATGGGCTACAGGCTTGTCACTC-3', Cox-2 forward 5'-CCCTTGGGTGTCAAAGGTAA-3', Cox-2 reverse 5'-GCCCTCGCTTATGATCTGTC-3'.

2.5. Co-immunoprecipitation.

For Co-immunoprecipitation experiments in BV-2 microglia, cells were plated in 15 cm dishes and then lysed with 1.5 ml of a modified lysis buffer (50 mM Tris HCL,150 mM NaCl, 6mM MgCl2, 1% NP 40) containing protease/phosphatase inhibitor cocktail (Cell Signaling). Cell lysate was left for 30 minutes on ice and subsequently centrifuged at 27,216 G (15,000 RPM) for 10 Minutes at 4°C. Cell lysates were incubated with either GDP (10 μM) alone or with GDP + $AlCl_3$ (100 μm) + NaF (10 mM) at 20 °C with gentle shaking for 30 minutes. Next, 2 μg of Gαi3 antibody (Santa Cruz) or normal rabbit IgG (Santa Cruz) was added. For Co-immunoprecipitation experiments in HEK-hTLR4293 cells were transfected prior to the co-immunoprecipitation with 0.25 μg of RGS10 WT, RGS10 E52K, and Gαi3. Following transfection, the co-immunoprecipitation was performed as described above.

2.6. PGE2 Measurement.

Molecular Pharmacology Fast Forward. Published on July 26, 2018 as DOI: 10.1124/mol.118.111674
This article has not been copyedited and formatted. The final version may differ from this version.

To quantify the levels of PGE2 in culture medium, BV-2 microglia culture medium was collected and centrifuged at 1,500 rpm for 10 min at 4°C. Enzyme-linked immunosorbent assay (ELISA) was performed using PGE2 ELISA kit (Enzo) to measure PGE2 levels in media following manufacturer's protocol.

2.7 CRISPR/Cas RGS10 knock out.

Mouse RGS10 sgRNA CRISPR/Cas9 All-in-One lentivector (K4107305) (gRNA Sequence: 49 TGTTTTGCAGATATCCATGA) and scrambled control vector (K010) were purchased from abm, Inc (Richmond, BC). Vectors (10ng) were transformed into Proclone™ competent DH5alpha cells and transformants were selected with 100ug/ml carbenicillin. All plasmids were isolated and the sequences were confirmed. Recombinant lentiviral particles were produced in 293T cells by packaging 10μg of expression sgRNA CRISPR/Cas9 vectors with 10 μg of amb's third generation (LV053) packaging mix according to company's lentivirus packaging protocol. Lentifectin™ transfection reagent (G074) was used in the transfection complex to facilitate DNA uptake by 293T cells. Transfection media was removed after 24 hours and replaced with complete growth media for additional 24 hours. Viral media was harvested 48 hours after transfection and centrifuged at 3000 rpm for 15 minutes at 4°C to pellet cell debris. Cleared supernatant was then filtered with a low-protein binding 0.45μM sterile filter and further concentrated by centrifugation at 25,000 rpm for 2 hours at 4°C (SW28 rotor of Beckman, ~120,000g). Viral pellets were resuspended and stored at -80 °C until transfection. Different volume of prepared lentivirus was transfected into BV2 cells in the presence of polybrene (0.8ug/ml). Media containing polybrene was replaced with complete culture media after 24 hours. 48 hours after transfection, cells were split and

Molecular Pharmacology Fast Forward. Published on July 26, 2018 as DOI: 10.1124/mol.118.111674
This article has not been copyedited and formatted. The final version may differ from this version.

transfectants were selected for stable expression using 6 μg/ml puromycin selection media, as determined by a kill curve. Genome editing was then assayed by western blotting and sequencing.

2.8 Experimental rigor and statistical analysis

All qRT-PCR data presented were performed in experimental and technical triplicates, except where indicated in Figure legends. Technical triplicates for each experiment were averaged prior to statistical analysis. All western images were quantified using densitometry of raw, unmodified image data, including background subtraction. Some images of western data have been modified slightly to adjust brightness, as indicated in legends. For analyzing data for statistical differences between groups, data were analyzed using analysis of variance (ANOVA) test followed by Tukey's multiple comparison tests. Statistical significance cutoff ranges indicated in figures correspond to: *$p < 0.05$ **$p < 0.01$ and ***$p < 0.001$.

3. Results

3.1 RGS10 knockdown elevates LPS-induced production of COX-2 and PGE2 in BV-2 microglia.

RGS10 has been shown to regulate expression of multiple inflammatory mediators following activation with lipopolysaccharide (LPS), but an effect on COX-2 has not been reported. Due to the essential roles of COX-2 in inflammation in microglia, we aimed to test whether LPS-stimulated COX-2 is also affected by RGS10 loss. We treated BV-2 microglia with RGS10-targeted siRNA or control siRNA for 24 hours before stimulating with LPS (10 ng/ml) for an additional 24 hours. Transient transfection of siRNA duplexes

Molecular Pharmacology Fast Forward. Published on July 26, 2018 as DOI: 10.1124/mol.118.111674
This article has not been copyedited and formatted. The final version may differ from this version.

in BV-2 cells consistently resulted in 50-70% reduction of RGS10 mRNA and protein levels, with no effect on mRNA expression of RGS2, a widely expressed RGS with high expression in microglia, or on mRNA expression of RGS12 and RGS14, which have highest sequence similarity to RGS10 (supplementary data Figure 1). As we have previously reported (Alqinyah et al., 2017), activation of microglia with LPS for 24 hours also suppressed RGS10 expression, and this suppression was additive with siRNA-mediated RGS10 suppression (Figure 1C). RGS10 knockdown significantly enhanced LPS-induced upregulation of COX-2 mRNA (**Figure 1A**). Similarly, LPS treatment resulted in higher levels of COX-2 protein in BV-2 cells, and this effect was significantly enhanced in cells transfected with RGS10 siRNA compared to control siRNA cells, suggesting that endogenous RGS10 suppresses COX-2 protein expression in BV-2 microglia (**Figure 1B, C**). One of the essential functions of COX-2 is the production of prostaglandins including PGE2, which is a critical mediator of neuroinflammation (Andreasson, 2010). Therefore, we tested the effect of RGS10 loss on LPS-induced production of PGE2 in BV-2 microglia. RGS10 knockdown enhanced LPS-stimulated release of PGE2 into microglia culture medium by approximately 25% (**Figure 1D**). Finally, to validate the results observed following transient siRNA-mediated knock-down, we generated BV-2 stable RGS10 knock-out cells using CRISPR-Cas9 as described in Methods. Complete suppression of RGS10 expression resulted in a robust amplification of LPS-stimulated COX-2 mRNA and protein levels (**Figure 1E-G**) Taken together, the results indicate that endogenous RGS10 regulates the expression of COX-2 and suppresses PGE2 release from microglia following LPS stimulation.

Molecular Pharmacology Fast Forward. Published on July 26, 2018 as DOI: 10.1124/mol.118.111674
This article has not been copyedited and formatted. The final version may differ from this version.

3.2 RGS10 acts as a classic GTPase-activating protein in microglia, but does not affect TLR4-induced acute signaling.

RGS10 deactivates Gαi proteins, and signaling cross-talk has been reported between Gαi pathways and LPS-stimulated toll-like receptors (TLRs) (Fan et al., 2007; Marty and Richard, 2010). Thus, we sought to determine whether the ability of RGS10 to regulate LPS-stimulated inflammatory signaling in microglia is mediated by RGS10 regulation of Gαi. First, we determined if LPS stimulation of BV-2 cells impacted association of RGS10 with Gα subunits in BV-2 cells. BV-2 cells were treated with 10 ng/mL of LPS for three hours, and then cell lysates were immunoprecipitated with Gαi, Gαq, or control antibodies and the associated proteins immunoblotted for the G proteins and RGS10. Multiple studies have described strong Gαi-selectivity of the RGS10 RGS domain (Ajit and Young, 2005; Taylor et al., 2016); however, it has also been reported that RGS10 can display weak interactions with Gαq (Soundararajan et al., 2008). Our results show that LPS activation of BV-2 cells enhances RGS10 association with Gαi, but no detectable association with Gαq was observed (**Figure 2A**). Next, we aimed to confirm that RGS10 expressed in BV-2 microglia can act as a Gαi GAP by assessing binding between RGS10 and transition state Gαi. This conformation of Gα subunits is the high affinity substrate for RGS domain GAP activity and is mimicked and stabilized in the presence of GDP with aluminum fluoride (AlF_4^-), while Gα-GDP has low affinity for RGS domains (Berman et al., 1996; Tesmer et al., 1997). BV-2 cell lysates were immunoprecipitated with Gαi3 or Gαq targeted antibody or control IgG in the presence of GDP or GDP plus AlF_4^-. Our results revealed a strong and distinct binding between RGS10 and Gαi3-AlF_4^-, with no detectable binding between RGS10 and Gαi3-GDP or

between RGS10 and either form of Gαq **(Figure 1B)**. Therefore, consistent with the literature, endogenous RGS10 appears to function as a Gi-selective GAP in BV-2 microglia.

GPCRs and TLRs both activate ERK and AKT kinase cascades as well as the transcription factor NFκB, and these pathways facilitate signaling crosstalk between the two receptor classes and downstream inflammatory signaling (Dauphinee et al., 2011; Fan et al., 2004; Ye, 2001). Given the ability of RGS10 to deactivate Gαi and the ability of Gαi pathways to activate ERK, AKT, and NFκB, we predicted that RGS10 regulation of TLR4-induced COX-2 and PGE2 production may be mediated by RGS10 deactivation of Gαi proteins that impact the ability of TLR4 to initiate these pathways. To explore this hypothesis further, we tested LPS-induced phosphorylation of p42/44 ERK with or without RGS10 knockdown. RGS10 knockdown had no effect on ERK phosphorylation following 20 minutes of LPS treatment (**Figure 2C**). Similarly, acute LPS treatment stimulated phosphorylation of AKT and p38 in BV-2 microglia, but RGS10 knockdown had no effect on these responses (data not shown). Phosphorylation of NFκB subunit p65, an early event in the NFκB activation cascade, was also significantly enhanced by LPS treatment, but this response was not affected by RGS10 knockdown (**Figure 2D**). Therefore, endogenous RGS10 appears to function as a Gαi GAP, but does not regulate acute LPS-stimulated signaling pathways that are co-regulated by Gαi.

3.3. The effect of Gαi inhibition on RGS10 knockdown-induced enhancement of TLR4 signaling.

Molecular Pharmacology Fast Forward. Published on July 26, 2018 as DOI: 10.1124/mol.118.111674
This article has not been copyedited and formatted. The final version may differ from this version.

To further explore the role of Gαi in RGS10's effects on inflammatory signaling, we next sought to determine whether enhanced COX-2 expression resulting from RGS10 knockdown is the result of amplified Gαi signaling. If the primary mechanism by which RGS10 regulates LPS stimulated inflammatory signaling is through regulation of Gαi GAP activity, then the effects of RGS10 knockdown should be reversed by inhibition of Gαi. To test this prediction, we measured the expression of COX-2 mRNA after LPS treatment and RGS10 knockdown with or without pretreatment with the Gi/o family inhibitor pertussis toxin (Ptx). Surprisingly, the RGS10 siRNA-mediated increase in LPS-stimulated COX-2 mRNA production (**Figure 3A**) or protein levels (**Figure 3B**) was completely resistant to pertussis toxin pretreatment. Since RGS10 loss has also been shown to enhance the production of the inflammatory cytokine TNFα, we further tested whether RGS10 knockdown-induced increase in TNFα expression was sensitive to Gαi inhibition. Like COX-2, the increase in LPS-stimulated TNFα expression mediated by RGS10 knockdown was not affected by Ptx (**Figure 3C**). To ensure that the dose of Ptx used is fully efficacious in BV-2 cells, we confirmed that Ptx completely blocked CXCL12 stimulated AKT phosphorylation, which has been shown to be mediated by Gαi signaling (Kumar et al., 2012) (**Figure 3D**). Collectively, these data suggest that RGS10 knockdown-mediated amplification of COX-2 and TNFα expression is not mediated by enhanced Gαi signaling.

3.4. Evaluating HEK293-hTLR4 cells as a model to study the effect of RGS10 on TLR4-induced inflammatory signaling

To more directly test the possibility that RGS10 regulates LPS-stimulated inflammatory signaling through a GAP-independent mechanism, we sought to assess whether

Molecular Pharmacology Fast Forward. Published on July 26, 2018 as DOI: 10.1124/mol.118.111674
This article has not been copyedited and formatted. The final version may differ from this version.

RGS10 G protein binding activity is required for this effect by comparing the effects of exogenous wildtype and GAP-deficient RGS10. BV-2 microglia cells are not an appropriate model for this experiment due to their low transfection efficiency and high levels of endogenous RGS10. As an alternative, we utilized HEK293-hTLR4 cells because they are easy to transfect, express low endogenous RGS10 levels, and stably overexpress TLR4 receptors. To confirm that this cell line is responsive to LPS treatment, we treated HEK293-hTLR4 cells with LPS (10 ng/ml), a dose that potently activates TLR4 signaling in BV-2 microglia. LPS caused a dramatic increase in TNFα mRNA levels (**Figure 4A**), and phosphorylation of p65-NFκB and p44/42 MAPK (data not shown) in HEK293-hTLR4 cells. However, COX-2 expression was not affected by LPS treatment in these cells, demonstrating that not all downstream TLR4 signaling pathways observed in BV-2 microglia will be recapitulated in HEK293-hTLR4 Cells. Nonetheless, the cells provided a suitable platform to assess the effect of exogenous RGS10 on LPS-induced production of TNFα. To address this question, we overexpressed wildtype RGS10 via transient plasmid transfection, inducing robust expression of exogenous RGS10 mRNA and protein. RGS10 overexpression suppressed LPS-induced production of TNFα after 24 hours of LPS treatment (**Figure 4A).** In contrast, RGS10 overexpression had no effect on acute LPS-induced activation of ERK and NFκB (data not shown). Finally, to determine if this effect is shared among closely related RGS domains, we overexpressed the RGS domain of RGS14 and compared the effect on LPS stimulated TNFα expression. Exogenous RGS14 RGS domain, when expressed at similar levels to exogenous RGS10, did not have any effect on LPS stimulated TNFα expression (**Figure 4B**). These results suggest that RGS10

Molecular Pharmacology Fast Forward. Published on July 26, 2018 as DOI: 10.1124/mol.118.111674
This article has not been copyedited and formatted. The final version may differ from this version.

regulates TLR4-stimulated gene expression to a greater extent than homologous RGS domains.

3.5. The effect of RGS10 WT and E52K mutant on TLR4-induced signaling in HEK293-hTLR4 cells.

We generated a single amino acid mutation E52K in RGS10 corresponding to a previously characterized GAP-dead mutation in the RGS domain of RGS12 (Sambi et al., 2006). To confirm that the mutation did not affect expression or protein stability, we compared RGS10 protein levels 48 hours after transient transfection with plasmid encoding RGS10 WT or RGS10 E52K in HEK293-hTLR4 cells. Our results indicate that the RGS10E52K mutant was expressed equally to the wild type (**Figure 5A**). To confirm that RGS10 E52K mutant is indeed unable to bind the active form of G proteins, we transfected HEK293-hTLR4 cells with wildtype and E52K RGS10 and performed co-immunoprecipitation to compare their G protein binding abilities. Only RGS10WT, and not E52K mutant, was able to bind active Gαi3-GDP-AlF_4^- (**Figure 5B**), which confirms that RGS10 E52K mutant has deficient GAP activity. Next, we aimed to confirm that the RGS10 GAP-deficient mutant lost the ability to suppress Gi-mediated signaling pathways. Unfortunately, comparing the effect of overexpressed wildtype and mutant RGS10 on GPCR-evoked Gi signaling in HEK293-hTLR4 cells was not possible, because we have not observed any effect of exogenous wildtype RGS10 overexpression on signaling stimulated by specific Gi-coupled GPCRs, including multiple purinergic, lysophospholipid, and chemokine receptor agonists tested (data not shown). It is possible that RGS10 regulates Gi mediated signaling downstream of select GPCRs which we have not yet tested. However, it is also possible that, although

Molecular Pharmacology Fast Forward. Published on July 26, 2018 as DOI: 10.1124/mol.118.111674
This article has not been copyedited and formatted. The final version may differ from this version.

RGS10 can interact with activated Gi in cell lysates, it does not function to regulate acute signaling following activation of cell-surface GPCRs. To indirectly address the effect of the EK mutant on signaling, we turned to the SKOV-3 cells, in which we have shown that exogenous RGS10 overexpression regulates basal ERK map kinase activity in the presence of serum. In these cells, overexpression of wildtype RGS10, but not EK mutant RGS10, suppressed ERK phosphorylation (**Figure 5C**), suggesting that this mutant is defective in regulating G protein signaling pathways.

Finally, we compared the ability of wildtype and GAP-dead E52K RGS10 to suppress LPS-induced TNFα mRNA in HEK293-hTLR4 cells. In sharp contrast to the lack of Gαi interaction activity of RGS10 E52K, we show that overexpression of both RGS10 WT and E52K mutant resulted in a similar inhibition of LPS-induced production of TNFα (**Figure 5D**). RGS10 mRNA was measured in parallel with TNFα in each experiment to ensure equivalent transfection efficiency of RGS10WT and E52K. These data provide further compelling evidence that RGS10 inhibits TLR4 signaling in a mechanism independent of its G protein interaction and GTPase accelerating activity.

3.6. Loss of RGS10 enhances TNFα and COX-2 expression in ovarian cancer cells, and this effect is mediated via a Gαi-independent mechanism.

The previous data demonstrate RGS10 suppression of the inflammatory cytokine TNFα and the inflammatory enzyme COX-2 in microglia. However, RGS10 has also been shown to play important roles in other physiological systems, most notably in ovarian cancer cells (Ali et al., 2013; Hooks et al., 2010). RGS10 suppresses survival signaling and maintains sensitivity to chemotherapeutic induced cell death in these cells, but the mechanism is unknown and has not been directly linked to a Gαi mediated pathway.

Molecular Pharmacology Fast Forward. Published on July 26, 2018 as DOI: 10.1124/mol.118.111674
This article has not been copyedited and formatted. The final version may differ from this version.

Inflammatory signaling including COX-2 and TNFα mediated pathways are directly linked to ovarian cancer chemoresistance (Gu et al., 2008; Symowicz et al., 2005). Based on our previous results demonstrating that RGS10 regulates the expression of both COX-2 and TNFα in microglia, we aimed to test whether RGS10 also regulates inflammatory mediators in ovarian cancer, and if so whether RGS10 also functions in a G protein-independent mechanism in ovarian cancer cells. We transfected SKOV-3 ovarian cancer cells with RGS10 siRNA or control siRNA in the presence or absence of Ptx, and assessed mRNA levels of COX-2 and TNFα. SKOV-3 cells transfected with RGS10 siRNA produced significantly higher levels of COX-2 (**Figure 6A**) and TNFα (**Figure 6B**) mRNA compared to cells transfected with control siRNA. SKOV-3 cells did not require receptor stimulation to observe an effect of RGS10 knockdown on COX-2 or TNFα expression, and these cells did not respond to LPS treatment with enhanced COX-2 or TNFα expression. As observed in microglia, Ptx treatment had no effect on RGS10 siRNA-mediated upregulation of COX-2 and TNFα expression. Successful knockdown of RGS10 following siRNA transfection in SKOV-3 cells was confirmed by RT-PCR (**Figure 6C**), and we confirmed that the dose of Ptx used in the experiment was sufficient to fully inhibit LPA-mediated ERK phosphorylation in SKOV-3, an established Gαi-mediated event (**Figure 6D**) (Hurst et al., 2008). These results demonstrate for the first time that RGS10 regulates inflammatory signaling pathways in ovarian cancer cells and demonstrate that RGS10 anti-inflammatory actions and mechanisms are not exclusive to immune cells but extend to other models. These findings provide new insight in understanding the mechanisms by which RGS10 suppresses chemoresistance and survival of ovarian cancer cells.

Molecular Pharmacology Fast Forward. Published on July 26, 2018 as DOI: 10.1124/mol.118.111674
This article has not been copyedited and formatted. The final version may differ from this version.

4. Discussion

RGS10 regulates cellular physiology and fundamental signaling pathways in microglia (Lee et al., 2011; Lee et al., 2008), macrophages (Lee et al., 2013), T-lymphocytes (Lee et al., 2016), neurons (Lee et al., 2012), osteoclasts (Yang et al., 2007; Yang et al., 2013; Yang and Li, 2007), cardiomyocytes (Miao et al., 2016), platelets (Hensch et al., 2016; Hensch et al., 2017), and cancer cells (Ali et al., 2013; Cacan et al., 2014; Hooks et al., 2010; Hooks and Murph, 2015). However, despite its small size and seemingly simple function as a G protein GAP, the molecular mechanisms accounting for RGS10 effects have not been defined. The results presented here significantly expand our understanding of the scope and mechanism of RGS10 regulation of inflammatory signaling. First, we show for the first time that RGS10 regulates COX-2 expression and subsequent prostaglandin production. Given the essential role of COX-2 and PGE2 in the physiology of diverse systems, this finding expands the potential relevance of RGS10 in physiology and disease. Further, our results provide the first evidence of regulation of inflammatory signaling pathways in cancer cells by RGS10, establishing a potential explanation for the effect of RGS10 on ovarian cancer cell survival. Finally, and most importantly, our results demonstrate that the effect of RGS10 on inflammatory signaling in both microglia and ovarian cancer cells cannot be explained by the ability of RGS10 to suppress Gαi signaling. We further show that exogenously expressed GAP-deficient RGS10 suppresses LPS-stimulated TNFα to the same extent as wildtype RGS10. This surprising result suggests novel RGS10 mechanisms and potentially novel binding partners linking RGS10 to inflammatory signaling mediators TNFα and COX-2.

Molecular Pharmacology Fast Forward. Published on July 26, 2018 as DOI: 10.1124/mol.118.111674
This article has not been copyedited and formatted. The final version may differ from this version.

RGS10 is highly expressed in microglia and RGS10 has profound effects on microglial function. Microglia are resident macrophages of the central nervous system and normally function to eliminate pathogens and debris (Kettenmann et al., 2011). However, chronic activation of these cells leads to amplified production of inflammatory cytokines, prostaglandins, and other neurotoxic molecules, ultimately resulting in significant neuronal death and neurodegenerative diseases (Lull and Block, 2010). Microglial RGS10 suppresses the release of TNFα and other inflammatory cytokines following inflammatory triggers (Lee et al., 2008) and plays a protective role against microglia-induced neurodegeneration of dopaminergic neurons (Lee et al., 2011). Reciprocally, microglial activation by either LPS or TNFα suppresses the expression of RGS10 and reduces RGS10 protein levels by approximately 50-70% for approximately 48 hours (Alqinyah et al., 2017). Thus, endogenous RGS10 silencing mechanisms likely serve to amplify and enhance inflammation in a feed-forward mechanism that sustains a continuous cycle of RGS10 suppression and enhanced production of inflammatory cytokines (Alqinyah et al., 2017; Lee et al., 2008). Importantly, the magnitude and duration of RGS10 suppression induced by transient siRNA transfection recapitulates that observed during suppression of RGS10 expression induced by endogenous activation of microglia (Alqinyah et al., 2017), suggesting that the effects reported here following siRNA knockdown will likely serve to amplify the magnitude of COX-2 and PGE2 signaling during endogenous microglial activation.

COX-2 enhances neuroinflammation and is implicated in microglia-induced neurotoxicity. To further assess inflammatory pathways regulated by RGS10 in microglia, we tested the effect of RGS10 loss on the expression of COX-2 and

production of PGE2. RGS10 knockdown enhanced LPS-induced production of COX-2 and the subsequent release of PGE2 from BV-2 microglia. These findings confirm previous reports demonstrating the anti-inflammatory roles of RGS10 in microglia, and further expands the scope of this effect. COX-2 and PGE2 have been shown to enhance neurodegeneration of dopaminergic neurons (Sanchez-Pernaute et al., 2004; Teismann et al., 2003). Therefore, it is possible that the effect of RGS10 on COX-2 and PGE2 production accounts, fully or partially, for the neuroprotective properties of RGS10 on dopaminergic neurons (Lee et al., 2008). Further, since COX-2 and PGE2 play diverse roles in the central nervous system, it is likely that RGS10 serves additional functions in central nervous system related to COX-2 regulation.

Remarkably, the mechanisms by which RGS10 exerts its anti-inflammatory and neuroprotective actions have not been defined. RGS proteins classically function to accelerate the inactivation of heterotrimeric G proteins, thereby inhibiting G protein-mediated signaling pathways (Watson et al., 1996). Indeed, RGS10 has been shown to function as a bona fide GAP with specificity to Gαi subunits (Hunt et al., 1996), and our data confirm that endogenous RGS10 in microglia does bind transition state Gαi, consistent with its classic GAP function. Gαi has been shown to enhance LPS-induced activation of multiple acute signaling pathways, including AKT and ERK kinase cascades (Dauphinee et al., 2011; Fan et al., 2004), as well as NFκB signaling, which is an essential pathway regulating the production of inflammatory cytokines (Ye, 2001). We also how that LPS stimulation of BV-2 cells enhances RGS10 interaction with Gαi. Therefore, our initial hypothesis was that RGS10, via its classic GTPase accelerating activity on Gαi, would suppress these acute signaling pathways following LPS

Molecular Pharmacology Fast Forward. Published on July 26, 2018 as DOI: 10.1124/mol.118.111674
This article has not been copyedited and formatted. The final version may differ from this version.

treatment. However, RGS10 knockdown had no effect on LPS-induced acute activation of ERK, AKT, or NFκB. This suggested the possibility that RGS10 may function in a mechanism that is independent of its effect on Gαi.

Our data also revealed that the amplified TNFα and COX-2 production observed with RGS10 knockdown was not altered by Gαi inhibition with pertussis toxin. While Ptx is an established and commonly used inhibitor of Gαi, it can produce G protein-independent effects (Mangmool and Kurose, 2011). To more rigorously assess the role of Gαi in RGS10 function, we created a RGS10 mutant E52K construct, based on a previously characterized GAP-dead RGS12 construct (Sambi et al., 2006). Overexpression studies comparing RGS10 E52K and wildtype RGS10 were performed in HEK293-hTLR4 cells, which stably express TLR4, MD-2 and CD14 co-receptor genes to recapitulate functional TLR4 signaling. Indeed, we confirmed that HEK293-hTLR4 cells show dramatically enhanced TNFα expression and activation of NFκB and ERK phosphorylation in response to LPS treatment with similar dose response as BV-2 cells. We demonstrated that overexpression of GAP-deficient mutant RGS10 suppressed LPS-induced TNFα to the same degree as wild type, suggesting that Gαi interaction is not required for the ability of RGS10 to inhibit TLR4 signaling. These data, combined with the observation that RGS10 regulation of LPS stimulated TNFα and COX-2 is Ptx insensitive in BV-2 microglia cells, strongly suggest that RGS10 anti-inflammatory effects are mediated by G protein-independent mechanisms. Further, we have validated the RGS10E52K mutant as a valuable tool to assess the role of RGS10 GAP activity in mediating the overall functions of RGS10.

In addition to its anti-inflammatory effects in microglia and macrophages, RGS10 has also been shown to regulate ovarian cancer cell survival and chemosensitivity. We have previously postulated that the ability of RGS10 to regulate cell survival in ovarian cancer cells was based on its ability to regulate signaling through Gi-coupled receptors for growth factors such as lysophosphatidic acid (LPA), a well-established autocrine survival factor that is upregulated in ovarian cancer (Hurst et al., 2008). However, while RGS10 suppression enhanced cell survival and basal AKT signaling, it did not enhance LPA-stimulated AKT or ERK signaling in our previous studies (Hooks et al., 2010). Our current observations demonstrate that RGS10 suppression strongly enhances basal TNFα and COX-2 expression in SKOV-3 ovarian cancer cells, indicating that RGS10 suppresses the production of inflammatory mediators in both immune and non-immune cells. As observed in BV-2 microglia, Gαi inhibition had no effect on RGS10 knockdown-induced upregulation of COX-2 and TNFα in SKOV-3. TNFα and COX-2 are strongly implicated in the development of chemoresistance and control of cell survival of many cancers including ovarian cancer, suggesting that these pathways may mediate the effect of RGS10 on chemoresistance (Greenhough et al., 2009; Kulbe et al., 2007). Further studies are warranted to determine if the ability of RGS10 to regulate inflammatory signaling in cancer cells fully accounts for its effects on chemoresistance, and if this mechanism extends to other cancer types.

The notion of GAP-independent mechanisms for RGS proteins is not new, and has been described in multiple RGS family members (see review: (Sethakorn et al., 2010)). However, many of these RGS proteins possess, in addition to RGS domains, additional domains that mediate some of these GAP-independent functions. For example, RGS12

Molecular Pharmacology Fast Forward. Published on July 26, 2018 as DOI: 10.1124/mol.118.111674
This article has not been copyedited and formatted. The final version may differ from this version.

and RGS14, the RGS family members most closely related to RGS10, interact with RAS and MEK2 proteins via RBD and PDZ domains respectively to perform multiple GAP-independent functions (Willard et al., 2007). In contrast, RGS10 contains only the conserved RGS domain and short disordered N- and C-terminal extensions containing sites for regulatory modifications, but no defined functions. This suggests that the RGS domain itself may mediate the GAP-independent function of RGS10. Indeed, G protein independent interactions and associations have been mapped to the RGS domains of multiple RGS proteins (Nguyen et al., 2009; Popov et al., 2000; Sethakorn et al., 2010), supporting the notion that the RGS domain is much more than just a GAP for G proteins. Structural studies have identified modest differences in the structure and flexibility of the RGS10 RGS domain, compared to other family members, which may allow distinct binding interactions (Soundararajan et al., 2008). Therefore, we predict that G protein-independent mechanisms and binding partners facilitate a significant subset of RGS10 functions. Identification and delineation of these novel molecular mechanisms is a critical next step in understanding RGS10 function, and will facilitate strategic targeting of RGS10 in the diverse pathologies in which its function is implicated.

Acknowledgements: The authors would like to thank Dr. Jillian Hurst for assistance in generating the E52K RGS10 mutation.

Authorship Contributions:

Participated in research design: Alqinyah, Hooks

Conducted experiments: Alqinyah, Almutairi, Wendimu

Performed data analysis: Alqinyah, Almutairi, Wendimu, Hooks

Molecular Pharmacology Fast Forward. Published on July 26, 2018 as DOI: 10.1124/mol.118.111674
This article has not been copyedited and formatted. The final version may differ from this version.

Wrote or contributed to writing of the manuscript: Alqinyah, Hooks

References

Ajit SK and Young KH (2005) Analysis of chimeric RGS proteins in yeast for the functional evaluation of protein domains and their potential use in drug target validation. *Cellular signalling* **17**(7): 817-825.

Ali MW, Cacan E, Liu Y, Pierce JY, Creasman WT, Murph MM, Govindarajan R, Eblen ST, Greer SF and Hooks SB (2013) Transcriptional suppression, DNA methylation, and histone deacetylation of the regulator of G-protein signaling 10 (RGS10) gene in ovarian cancer cells. *PloS one* **8**(3): e60185.

Alqinyah M, Maganti N, Ali MW, Yadav R, Gao M, Cacan E, Weng HR, Greer SF and Hooks SB (2017) Regulator of G Protein Signaling 10 (Rgs10) Expression Is Transcriptionally Silenced in Activated Microglia by Histone Deacetylase Activity. *Mol Pharmacol* **91**(3): 197-207.

Andreasson K (2010) Emerging roles of PGE2 receptors in models of neurological disease. *Prostaglandins Other Lipid Mediat* **91**(3-4): 104-112.

Berman DM, Kozasa T and Gilman AG (1996) The GTPase-activating protein RGS4 stabilizes the transition state for nucleotide hydrolysis. *The Journal of biological chemistry* **271**(44): 27209-27212.

Bijman MN, Hermelink CA, van Berkel MP, Laan AC, Janmaat ML, Peters GJ and Boven E (2008) Interaction between celecoxib and docetaxel or cisplatin in human cell lines of ovarian cancer and colon cancer is independent of COX-2 expression levels. *Biochemical pharmacology* **75**(2): 427-437.

Blasi E, Barluzzi R, Bocchini V, Mazzolla R and Bistoni F (1990) Immortalization of murine microglial cells by a v-raf/v-myc carrying retrovirus. *Journal of neuroimmunology* **27**(2-3): 229-237.

Cacan E, Ali MW, Boyd NH, Hooks SB and Greer SF (2014) Inhibition of HDAC1 and DNMT1 modulate RGS10 expression and decrease ovarian cancer chemoresistance. *PloS one* **9**(1): e87455.

Dauphinee SM, Voelcker V, Tebaykina Z, Wong F and Karsan A (2011) Heterotrimeric Gi/Go proteins modulate endothelial TLR signaling independent of the MyD88-dependent pathway. *Am J Physiol Heart Circ Physiol* **301**(6): H2246-2253.

Fan H, Luttrell LM, Tempel GE, Senn JJ, Halushka PV and Cook JA (2007) β-Arrestins 1 and 2 differentially regulate LPS-induced signaling and pro-inflammatory gene expression. *Molecular immunology* **44**(12): 3092-3099.

Fan H, Peck OM, Tempel GE, Halushka PV and Cook JA (2004) Toll-like receptor 4 coupled GI protein signaling pathways regulate extracellular signal-regulated kinase phosphorylation and AP-1 activation independent of NFkappaB activation. *Shock* **22**(1): 57-62.

Greenhough A, Smartt HJ, Moore AE, Roberts HR, Williams AC, Paraskeva C and Kaidi A (2009) The COX-2/PGE2 pathway: key roles in the hallmarks of cancer and adaptation to the tumour microenvironment. *Carcinogenesis* **30**(3): 377-386.

Gu P, Su Y, Guo S, Teng L, Xu Y, Qi J, Gong H and Cai Y (2008) Over-expression of COX-2 induces human ovarian cancer cells (CAOV-3) viability, migration and proliferation in association with PI3-k/Akt activation. *Cancer Investigation* **26**(8): 822-829.

Hensch NR, Karim ZA, Druey KM, Tansey MG and Khasawneh FT (2016) RGS10 Negatively Regulates Platelet Activation and Thrombogenesis. *PloS one* **11**(11): e0165984.

Hensch NR, Karim ZA, Qasim H and Khasawneh FT (2017) RGS10 serves as a braking system for platelet hyperactivity. *The FASEB Journal* **31**(1 Supplement): 674.676-674.676.

Hooks SB, Callihan P, Altman MK, Hurst JH, Ali MW and Murph MM (2010) Regulators of G-Protein signaling RGS10 and RGS17 regulate chemoresistance in ovarian cancer cells. *Mol Cancer* **9**: 289.

Hooks SB and Murph MM (2015) Cellular deficiency in the RGS10 protein facilitates chemoresistant ovarian cancer. *Future Med Chem* **7**(12): 1483-1489.

Hunt TW, Fields TA, Casey PJ and Peralta EG (1996) RGS10 is a selective activator of G alpha i GTPase activity. *Nature* **383**(6596): 175-177.

Hurst JH, Henkel PA, Brown AL and Hooks SB (2008) Endogenous RGS proteins attenuate Galpha(i)-mediated lysophosphatidic acid signaling pathways in ovarian cancer cells. *Cellular signalling* **20**(2): 381-389.

Kettenmann H, Hanisch UK, Noda M and Verkhratsky A (2011) Physiology of microglia. *Physiol Rev* **91**(2): 461-553.

Kulbe H, Thompson R, Wilson JL, Robinson S, Hagemann T, Fatah R, Gould D, Ayhan A and Balkwill F (2007) The inflammatory cytokine tumor necrosis factor-alpha generates an autocrine tumor-promoting network in epithelial ovarian cancer cells. *Cancer Res* **67**(2): 585-592.

Kumar R, Tripathi V, Ahmad M, Nath N, Mir RA, Chauhan SS and Luthra K (2012) CXCR7 mediated Gialpha independent activation of ERK and Akt promotes cell survival and chemotaxis in T cells. *Cell Immunol* **272**(2): 230-241.

Lee JK, Chung J, Druey KM and Tansey MG (2012) RGS10 exerts a neuroprotective role through the PKA/c-AMP response-element (CREB) pathway in dopaminergic neuron-like cells. *Journal of neurochemistry* **122**(2): 333-343.

Lee JK, Chung J, Kannarkat GT and Tansey MG (2013) Critical Role of Regulator G-Protein Signaling 10 (RGS10) in Modulating Macrophage M1/M2 Activation. *PloS one* **8**(11): e81785.

Lee JK, Chung J, McAlpine FE and Tansey MG (2011) Regulator of G-protein signaling-10 negatively regulates NF-kappaB in microglia and neuroprotects dopaminergic neurons in hemiparkinsonian rats. *The Journal of neuroscience : the official journal of the Society for Neuroscience* **31**(33): 11879-11888.

Lee JK, Kannarkat GT, Chung J, Joon Lee H, Graham KL and Tansey MG (2016) RGS10 deficiency ameliorates the severity of disease in experimental autoimmune encephalomyelitis. *Journal of neuroinflammation* **13**: 24.

Lee JK, McCoy MK, Harms AS, Ruhn KA, Gold SJ and Tansey MG (2008) Regulator of G-protein signaling 10 promotes dopaminergic neuron survival via regulation of the microglial inflammatory response. *The Journal of neuroscience : the official journal of the Society for Neuroscience* **28**(34): 8517-8528.

Lull ME and Block ML (2010) Microglial activation and chronic neurodegeneration. *Neurotherapeutics* **7**(4): 354-365.

Mangmool S and Kurose H (2011) G(i/o) protein-dependent and -independent actions of Pertussis Toxin (PTX). *Toxins (Basel)* **3**(7): 884-899.

Marty C and Richard DY (2010) Heterotrimeric G protein signaling outside the realm of seven transmembrane domain receptors. *Molecular pharmacology* **78**(1): 12-18.

Miao R, Lu Y, Xing X, Li Y, Huang Z, Zhong H, Huang Y, Chen AF, Tang X, Li H, Cai J and Yuan H (2016) Regulator of G-Protein Signaling 10 Negatively Regulates Cardiac Remodeling by Blocking Mitogen-Activated Protein Kinase-Extracellular Signal-Regulated Protein Kinase 1/2 Signaling. *Hypertension* **67**(1): 86-98.

Minghetti L (2004) Cyclooxygenase-2 (COX-2) in inflammatory and degenerative brain diseases. *J Neuropathol Exp Neurol* **63**(9): 901-910.

Nguyen CH, Ming H, Zhao P, Hugendubler L, Gros R, Kimball SR and Chidiac P (2009) Translational control by RGS2. *J Cell Biol* **186**(5): 755-765.

Popov SG, Krishna UM, Falck JR and Wilkie TM (2000) Ca2+/Calmodulin reverses phosphatidylinositol 3,4, 5-trisphosphate-dependent inhibition of regulators of G protein-signaling GTPase-activating protein activity. *The Journal of biological chemistry* **275**(25): 18962-18968.

Sambi BS, Hains MD, Waters CM, Connell MC, Willard FS, Kimple AJ, Pyne S, Siderovski DP and Pyne NJ (2006) The effect of RGS12 on PDGFbeta receptor signalling to p42/p44 mitogen activated protein kinase in mammalian cells. *Cellular signalling* **18**(7): 971-981.

Sanchez-Pernaute R, Ferree A, Cooper O, Yu M, Brownell AL and Isacson O (2004) Selective COX-2 inhibition prevents progressive dopamine neuron degeneration in a rat model of Parkinson's disease. *J Neuroinflammation* **1**(1): 6.

Sethakorn N, Yau DM and Dulin NO (2010) Non-canonical functions of RGS proteins. *Cellular signalling* **22**(9): 1274-1281.

Soundararajan M, Willard FS, Kimple AJ, Turnbull AP, Ball LJ, Schoch GA, Gileadi C, Fedorov OY, Dowler EF, Higman VA, Hutsell SQ, Sundstrom M, Doyle DA and Siderovski DP (2008) Structural diversity in the RGS domain and its interaction with heterotrimeric G protein alpha-subunits. *Proceedings of the National Academy of Sciences of the United States of America* **105**(17): 6457-6462.

Symowicz J, Adley BP, Woo MM, Auersperg N, Hudson LG and Stack MS (2005) Cyclooxygenase-2 functions as a downstream mediator of lysophosphatidic acid to promote aggressive behavior in ovarian carcinoma cells. *Cancer Res* **65**(6): 2234-2242.

Taylor VG, Bommarito PA and Tesmer JJ (2016) Structure of the Regulator of G Protein Signaling 8 (RGS8)-Galphaq Complex: MOLECULAR BASIS FOR Galpha SELECTIVITY. *The Journal of biological chemistry* **291**(10): 5138-5145.

Teismann P, Tieu K, Choi DK, Wu DC, Naini A, Hunot S, Vila M, Jackson-Lewis V and Przedborski S (2003) Cyclooxygenase-2 is instrumental in Parkinson's disease neurodegeneration. *Proc Natl Acad Sci U S A* **100**(9): 5473-5478.

Tesmer JJ, Berman DM, Gilman AG and Sprang SR (1997) Structure of RGS4 bound to AlF4--activated G(i alpha1): stabilization of the transition state for GTP hydrolysis. *Cell* **89**(2): 251-261.

Watson N, Linder ME, Druey KM, Kehrl JH and Blumer KJ (1996) RGS family members: GTPase-activating proteins for heterotrimeric G-protein alpha-subunits. *Nature* **383**(6596): 172-175.

Willard MD, Willard FS, Li X, Cappell SD, Snider WD and Siderovski DP (2007) Selective role for RGS12 as a Ras/Raf/MEK scaffold in nerve growth factor-mediated differentiation. *EMBO J* **26**(8): 2029-2040.

Yang S, Chen W, Stashenko P and Li YP (2007) Specificity of RGS10A as a key component in the RANKL signaling mechanism for osteoclast differentiation. *J Cell Sci* **120**(Pt 19): 3362-3371.

Yang S, Hao L, McConnell M, Zhou X, Wang M, Zhang Y, Mountz JD, Reddy M, Eleazer PD and Li Y-P (2013) Inhibition of Rgs10 expression prevents immune cell infiltration in bacteria-induced inflammatory lesions and osteoclast-mediated bone destruction. *Bone research* **1**(3): 267.

Yang S and Li YP (2007) RGS10-null mutation impairs osteoclast differentiation resulting from the loss of [Ca2+]i oscillation regulation. *Genes Dev* **21**(14): 1803-1816.

Ye RD (2001) Regulation of nuclear factor kappaB activation by G-protein-coupled receptors. *J Leukoc Biol* **70**(6): 839-848.

Molecular Pharmacology Fast Forward. Published on July 26, 2018 as DOI: 10.1124/mol.118.111674
This article has not been copyedited and formatted. The final version may differ from this version.

Footnotes

a) Funding for this work was provided by the National Institutes of Health National Institute for Neurological Disorders and Stroke [Grant NS101161].

Molecular Pharmacology Fast Forward. Published on July 26, 2018 as DOI: 10.1124/mol.118.111674
This article has not been copyedited and formatted. The final version may differ from this version.

Figure 1. Loss of RGS10 enhances LPS-stimulated COX-2 expression and PGE2 production in BV-2 microglia

A. BV-2 microglia cells were plated in 6 well plates and simultaneously transfected with either control or RGS10 siRNA. Cells were cultured for 24 hours and then incubated with vehicle or LPS (10 ng/ml) for an additional 24 hours. RNA extraction, cDNA synthesis, qRT-PCR were performed as described in Methods. Expression of COX-2 mRNA was normalized to the control Actin, and relative expression levels were calculated by the $2^{-\Delta\Delta Ct}$ method. Data are analyzed from two independent experiments. The difference between groups was analyzed by ANOVA test followed by Tukey's test. Data are presented as Mean ± SEM where *$p < 0.05$ **$p < 0.01$ and ***$p < 0.001$. **B, C.** BV-2 microglia were plated in 24 well plates and transfected with control or RGS10 siRNA for 24 hours and then treated with vehicle or LPS for an additional 24 hours. Cells were lysed, and SDS-PAGE was performed followed by immunoblotting using specific antibodies against COX-2, RGS10, and the loading control GAPDH. B. The image is representative of two independent experiments. C. Images from two independent western experiments were quantified with densitometry**.** D. BV-2 microglia cells were plated in 6 well plates and simultaneously transfected with either control or RGS10 siRNA. Cells were cultured for 24 hours and then incubated with vehicle or LPS (10 ng/ml) for an additional 24 hours. Culture medium was collected and PGE2 levels were measured using ELISA. Conversion of raw absorbance values to pg/mL concentration was conducted using a standard curve following manufacturer's protocol. Data are analyzed from four independent experiments and difference between groups was analyzed by ANOVA test followed by Tukey's test. Data are presented as Mean ±

Molecular Pharmacology Fast Forward. Published on July 26, 2018 as DOI: 10.1124/mol.118.111674
This article has not been copyedited and formatted. The final version may differ from this version.

SEM where *p < 0.05. **E-G.** BV-2 cells were stably infected with control or RGS10-targeted CRISPR-Cas9 lentivirus as described in methods. Control and RGS10 knock-out cells were treated with 10 ng/mL LPS for 24 hours and then harvested for western blotting to assess COX-2, RGS10, and GAPDH protein levels. **E**: Representative image of two independent experiments**. F**: Quantification of densitometry from both independent experiments. **G**: In parallel, control and RGS10 knock-out BV-2 cells were treated with vehicle or LPS for 24 hours, and COX-2 and RGS10 mRNA levels were determined relative to actin control, as described.

Figure 2. Endogenous RGS10 associates with the active form of Gαi, but doesn't regulate ERK or NFκB phosphorylation

A. BV-microglia cells were plated in 15 cm dishes and treated with vehicle or 10 ng/mL LPS for 3 hours and then lysed using modified RIPA lysis buffer as described in Methods. Co-immunoprecipitation was performed using Gαi3, Gαq, or control IgG antibodies. Western blot analysis was conducted to probe for RGS10, Gαi3, or Gαq. B. BV-2 cell lysates were incubated with GDP (10 μM) alone or with AlF_4^- for 30 minutes at 25 °C and immunoprecipitated as above **C-D.** BV-2 microglia cells were plated in 24 well plates and transfected with control or RGS10 siRNA before incubation with vehicle or LPS for 20 minutes. Cells were lysed, and SDS-PAGE was performed followed by immunoblotting using specific antibodies against **C.** phospho-ERK, total ERK, RGS10, and the loading control GAPDH, and **D.** phospho-P65 NFκB, total P65 NFκB, RGS10 and GAPDH. **E**. Quantification of RGS10 protein levels in experiments shown in C-D was performed using densitometry. Combined data from two independent experiments were analyzed. (**A-D**). Images are representative of two independent experiments.

Molecular Pharmacology Fast Forward. Published on July 26, 2018 as DOI: 10.1124/mol.118.111674
This article has not been copyedited and formatted. The final version may differ from this version.

Figure3. PTX pretreatment does not affect RGS10 knockdown-induced increase of LPS stimulated COX-2 and TNFα

A) BV-2 microglia cells were plated in 6 well plates and transfected with either control or RGS10 siRNA. 24 hours after transfection, cells were incubated with vehicle or LPS (10 ng/ml) for 24 hours with or without pertussis toxin (100 ng/ml). Pertussis toxin was added 4 hours prior to LPS and included throughout the 24 hour LPS treatment. Expression of COX-2 mRNA was normalized to the endogenous control Actin, and relative expression was calculated by the $2^{-\Delta\Delta Ct}$ method. Data are analyzed from four independent experiments and difference between groups was analyzed by ANOVA test followed by Tukey's test. Data are presented as Mean ± SEM where *p < 0.05 **p < 0.01 and ***p < 0.001. **B)** BV-2 microglia cells were plated in 24 well plates and transfected with control or RGS10 siRNA. 24 hours after transfection, cells were treated with vehicle or LPS for an additional 24 hours with or without pertussis toxin (100 ng/ml). Pertussis toxin was added 4 hours prior to LPS and included throughout the 24 hour LPS treatment. Cells were lysed, and SDS-PAGE was performed followed by immunoblotting using specific antibodies against COX-2, RGS10, and the loading control GAPDH. Band intensity was analyzed from three independent experiments and difference between groups was analyzed by ANOVA test followed by Tukey's test. Data are presented as Mean ± SEM where *p < 0.05 **p < 0.01 and ***p < 0.001. **C)** BV-2 microglia cells were plated in 6 well plates and transfected with either control or RGS10 siRNA. After 24 hours, cells were incubated with vehicle or LPS (10 ng/ml) for an additional 24 hours with or without pertussis toxin (100 ng/ml). Pertussis toxin was added 4 hours prior to LPS and included throughout the 24 hour LPS treatment.

Molecular Pharmacology Fast Forward. Published on July 26, 2018 as DOI: 10.1124/mol.118.111674
This article has not been copyedited and formatted. The final version may differ from this version.

Expression of TNFα mRNA was normalized to the endogenous control Actin, and relative expression was calculated by the $2^{-\Delta\Delta Ct}$ method. Data are analyzed from five independent experiments and difference between groups was analyzed by ANOVA test followed by Tukey's test. Data are presented as Mean ± SEM where *p < 0.05 **p < 0.01 and ***p < 0.001. **D)** BV-2 microglia were plated in 24 well plates and then treated with vehicle or CXCL12 (200 ng/ml) for 5 minutes with or without a preincubation with pertussis toxin (100 ng/ml) overnight. Following incubation, cells were lysed, and SDS-PAGE was performed followed by immunoblotting using specific antibodies against phospho-AKT, total AKT, and GAPDH. The graph is a representative of two independent experiments.

Figure 4. HEK293-hTLR4 cells express TNFα in response LPS and express high levels of exogenous RGS10

A. HEK293-hTLR4 cells were plated in 24 wells plate and allowed to reach ~ 80% confluency. Cells were transfected with either empty vector or RGS10 plasmid for 48 hours and treated with vehicle or LPS 24 hours after transfection. mRNA expression of TNFα and RGS10 were normalized to the endogenous control Actin, and relative expression was calculated by the $2^{-\Delta\Delta Ct}$ method. **B**). HEK293-hTLR4 cells were transfected with empty vector or plasmid encoding RGS10 or the RGS domain of RGS14. RNA was isolated and TNFα expression assessed as above. Data are analyzed from three independent experiments each with technical duplicates and difference between groups was analyzed by ANOVA test followed by Tukey's test. Data are presented as Mean ± SEM where *p < 0.05 **p < 0.01 and ***p < 0.001.

Molecular Pharmacology Fast Forward. Published on July 26, 2018 as DOI: 10.1124/mol.118.111674
This article has not been copyedited and formatted. The final version may differ from this version.

Figure 5. Overexpression of wildtype and "GAP-dead" E52K RGS10 equally suppress LPS-induced TNFα expression

A. HEK293-hTLR4 cells were plated in 24 wells plate and allowed to reach approximately 80% confluency before transfection with 0.5 μg of RGS10 WT or RGS10 E52K plasmids. 48 hours after transfection, cells were lysed, and SDS-PAGE was performed followed by immunoblotting using specific antibodies against RGS10 and GAPDH. **B.** HEK293-hTLR4 cells were plated in 10 cm dishes and transfected with pcDNA encoding Gαi3 along with either RGS10 WT or RGS10 E52K plasmids. 48 hours after transfection, cells were lysed with modified lysis buffer and cell lysates were incubated with GDP (10 μM) alone or with AlF_4^-. Co-immunoprecipitation was performed using Gαi3 or control IgG antibodies. Western blot analysis was conducted to probe for RGS10 and Gαi3. **C.** SKOV-3 cells were transfected with empty vector or plasmid encoding wildtype RGS10 or E52K RGS10. Cell lysates were analyzed using SDS-PAGE and western blotting for phosphorylated p42/p44 ERK Map kinase and total p42/p44 ERK Map kinase. Each Map kinase signal was normalized to GAPDH, and the ratio of phospho/total Map kinase was calculated. D. HEK293-hTLR4 cells were plated in 24 well plates and transfected with RGS10 WT or RGS10 E52K plasmids for 48 hours. Cells were incubated with LPS (10 ng/ml) for 24 hours. mRNA expression of TNFα was normalized to the endogenous control Actin, and relative expression was calculated by the $2^{-\Delta\Delta Ct}$ method. **(A-B)** Images are representative of two independent experiments. **(C-D)** Data are analyzed from two independent experiments each with technical duplicates and difference between groups was analyzed by ANOVA test

Molecular Pharmacology Fast Forward. Published on July 26, 2018 as DOI: 10.1124/mol.118.111674
This article has not been copyedited and formatted. The final version may differ from this version.

followed by Tukey's test. Data are presented as mean ± SEM where *p < 0.05 **p < 0.01 and ***p < 0.001.

Figure 6: Knockdown of RGS10 significantly increases expression of COX-2 and TNFα via a Gi-independent mechanism in SKOV-3 ovarian cancer cells.

SKOV-3 cells were plated in a 6 well plate and transiently transfected with control or RGS10-targeted siRNA constructs. 20 hours after transfection, cells were treated with vehicle or Ptx (100ng/ml) for an additional 28 hours. RNA was isolated from cells using TRIzol reagent and cDNA was synthesized from the extracted RNA. COX-2 **(A)**, TNFα **(B)**, and RGS10 **(C)** transcript levels were quantified using quantitative RT-PCR and normalized to the housekeeping gene GAPDH. The relative expression was calculated by the $2^{-\Delta\Delta CT}$ method. Data in **(A-C)** are compiled from three independent experimental repeats. Data were analyzed for statistical differences using an analysis of variance (ANOVA) followed by Tukey's test between groups. Data are presented as Mean ± SEM where *: P<0.005, **: P<0.01, and ***: P<0.001 indicate the levels of significance. **(D)** SKOV-3 cells plated in 24 wells plate were serum-starved overnight with or without Ptx (100ng/ml) prior to treatment with vehicle or LPA (10 μM) for five minutes. Cells were lysed and subjected to SDS-PAGE and western blotting was performed using specific antibodies against phospho-ERK, total ERK, and GAPDH. Image is representative of two independent experiments, each performed in duplicates.

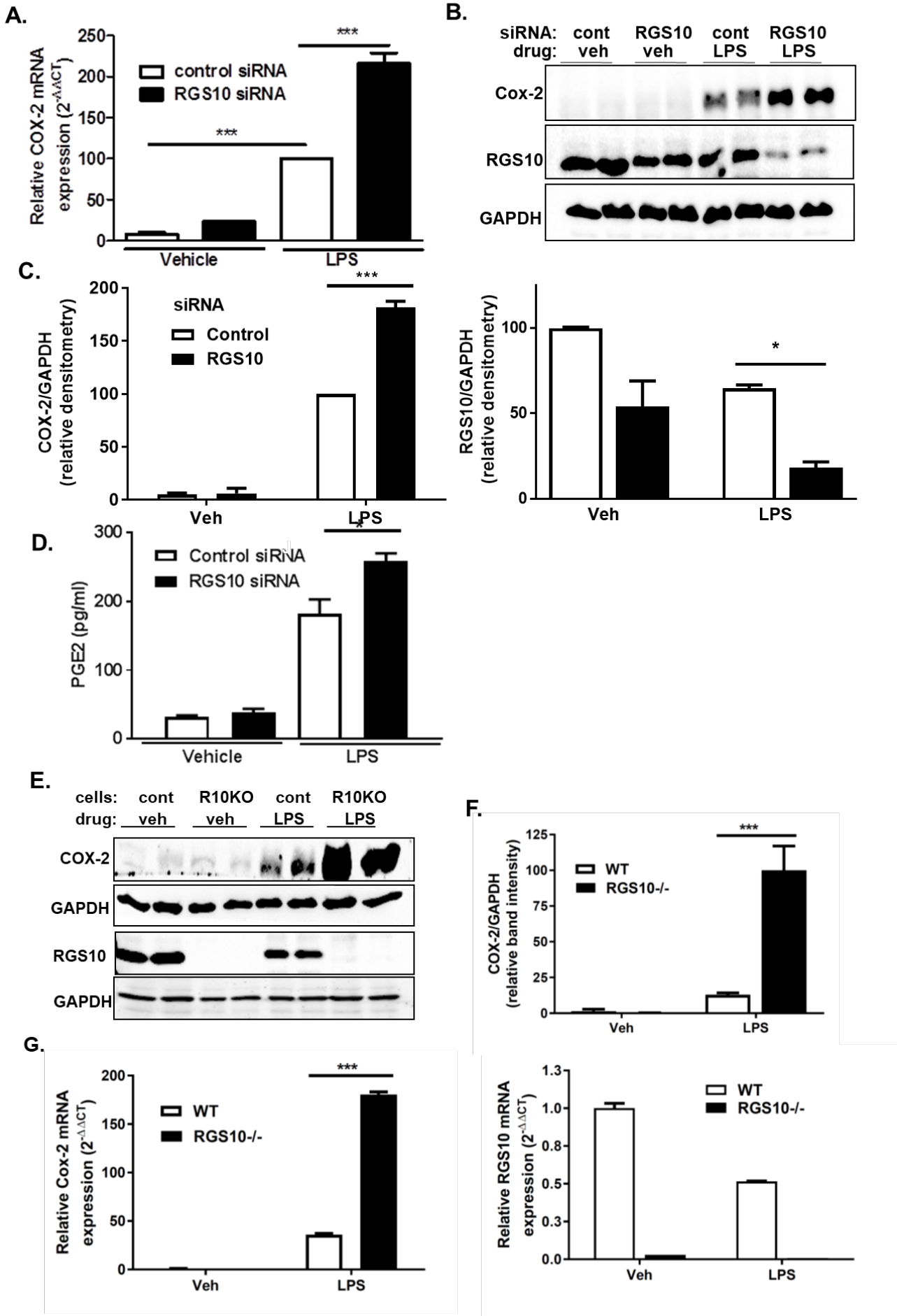

Figure 1

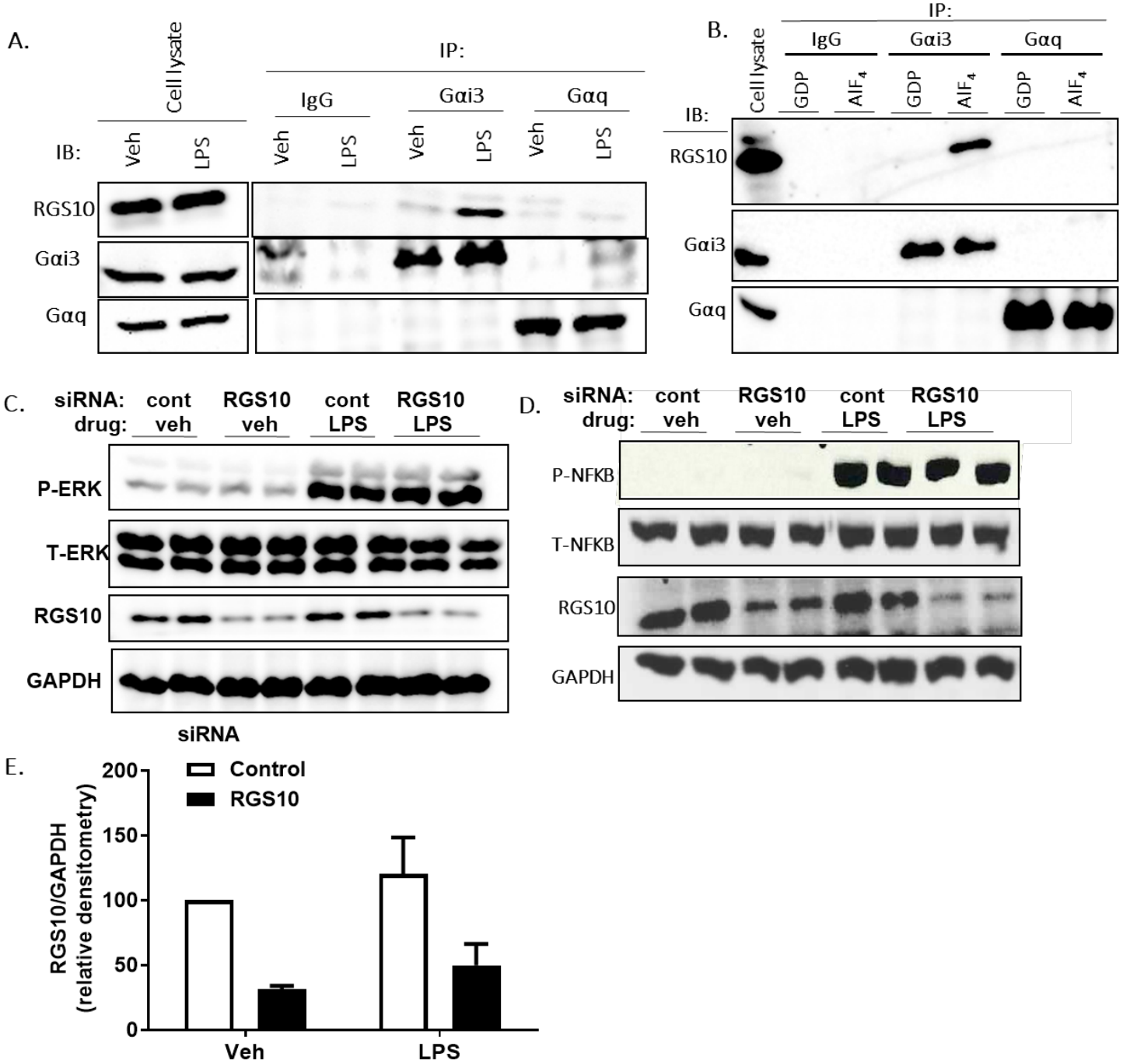

Figure 2

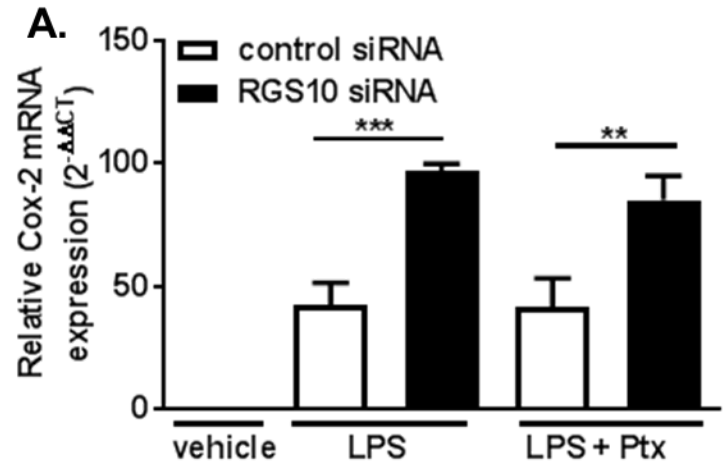

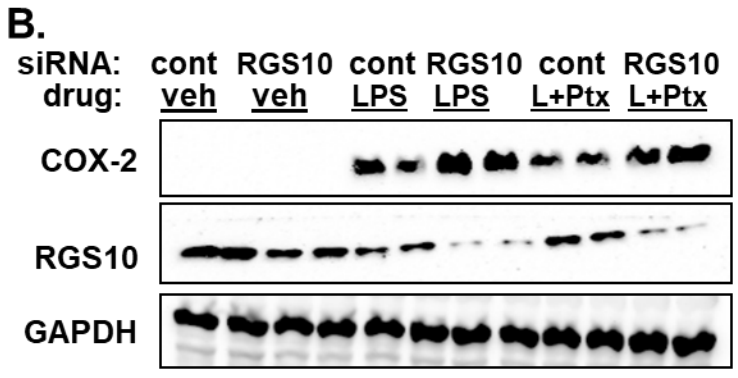

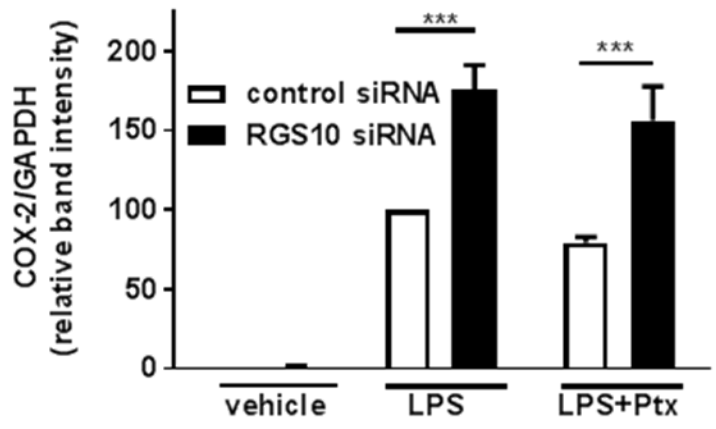

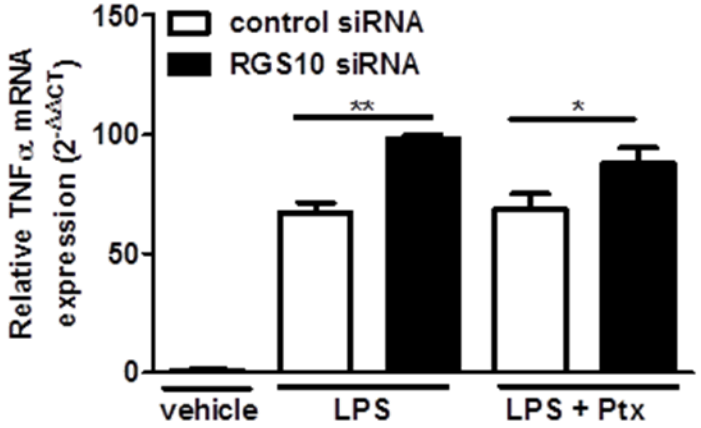

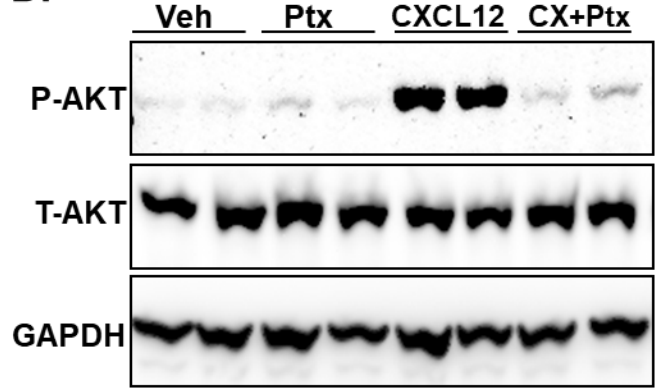

Figure 3

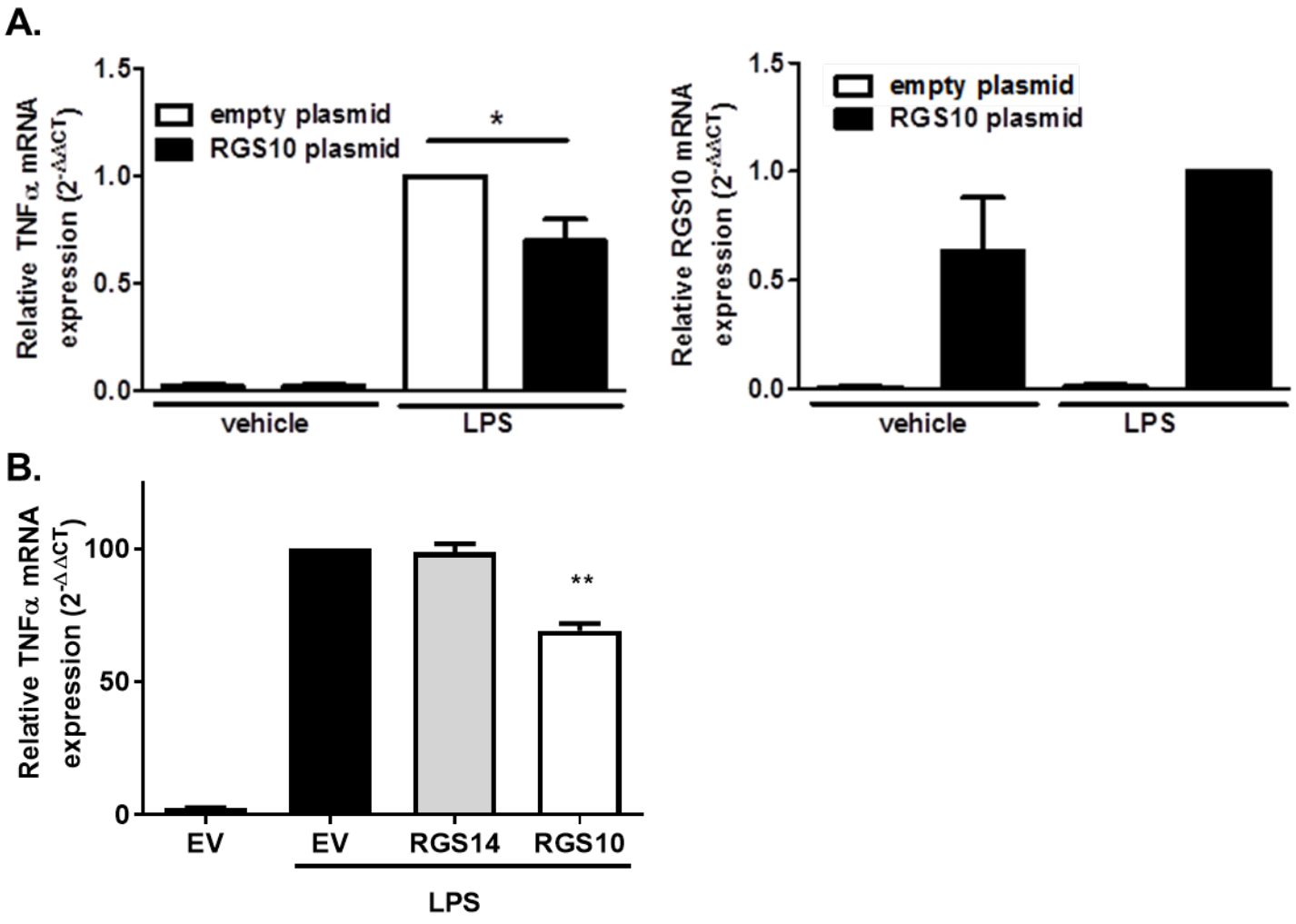

Figure 4

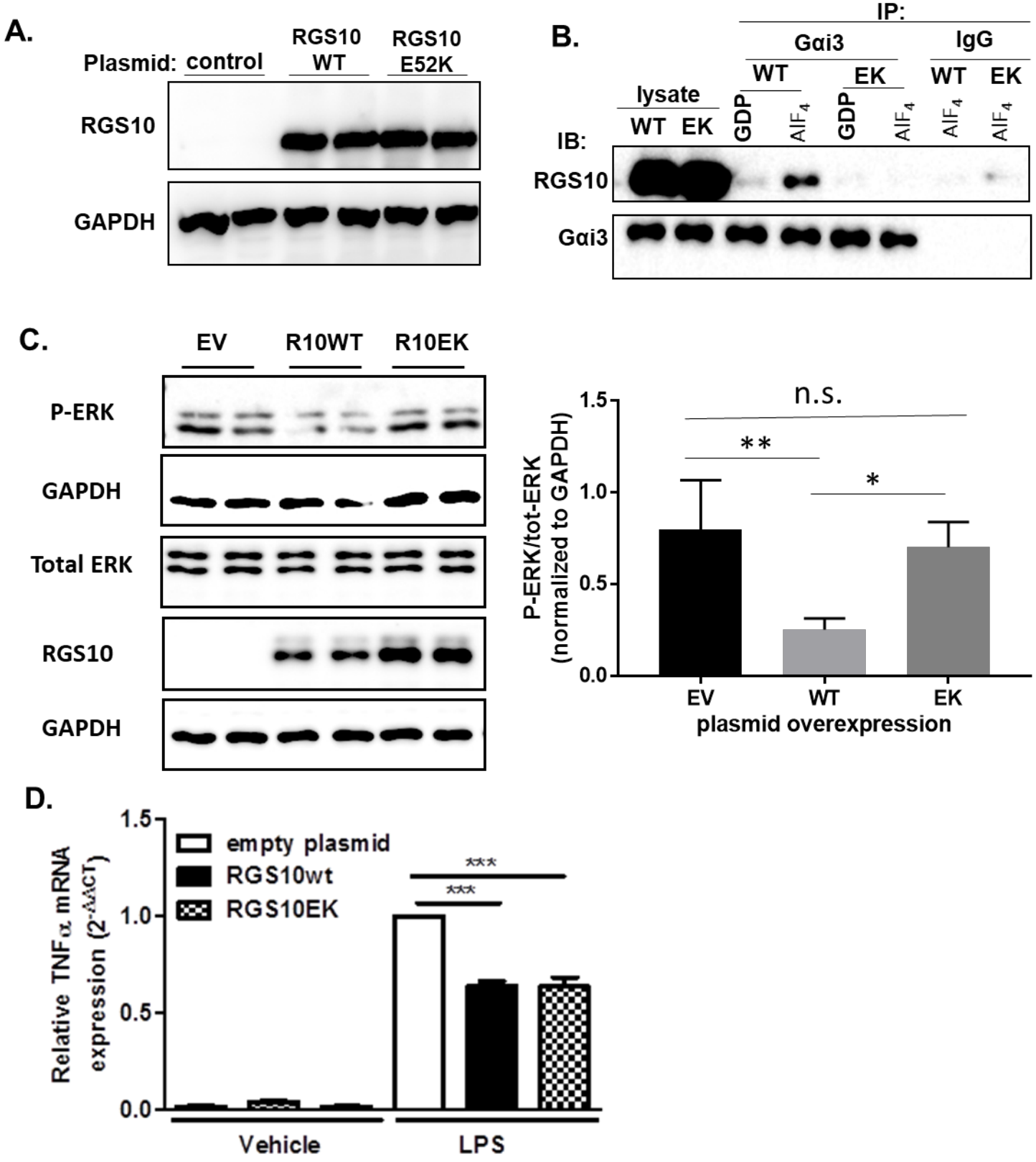

Figure 5

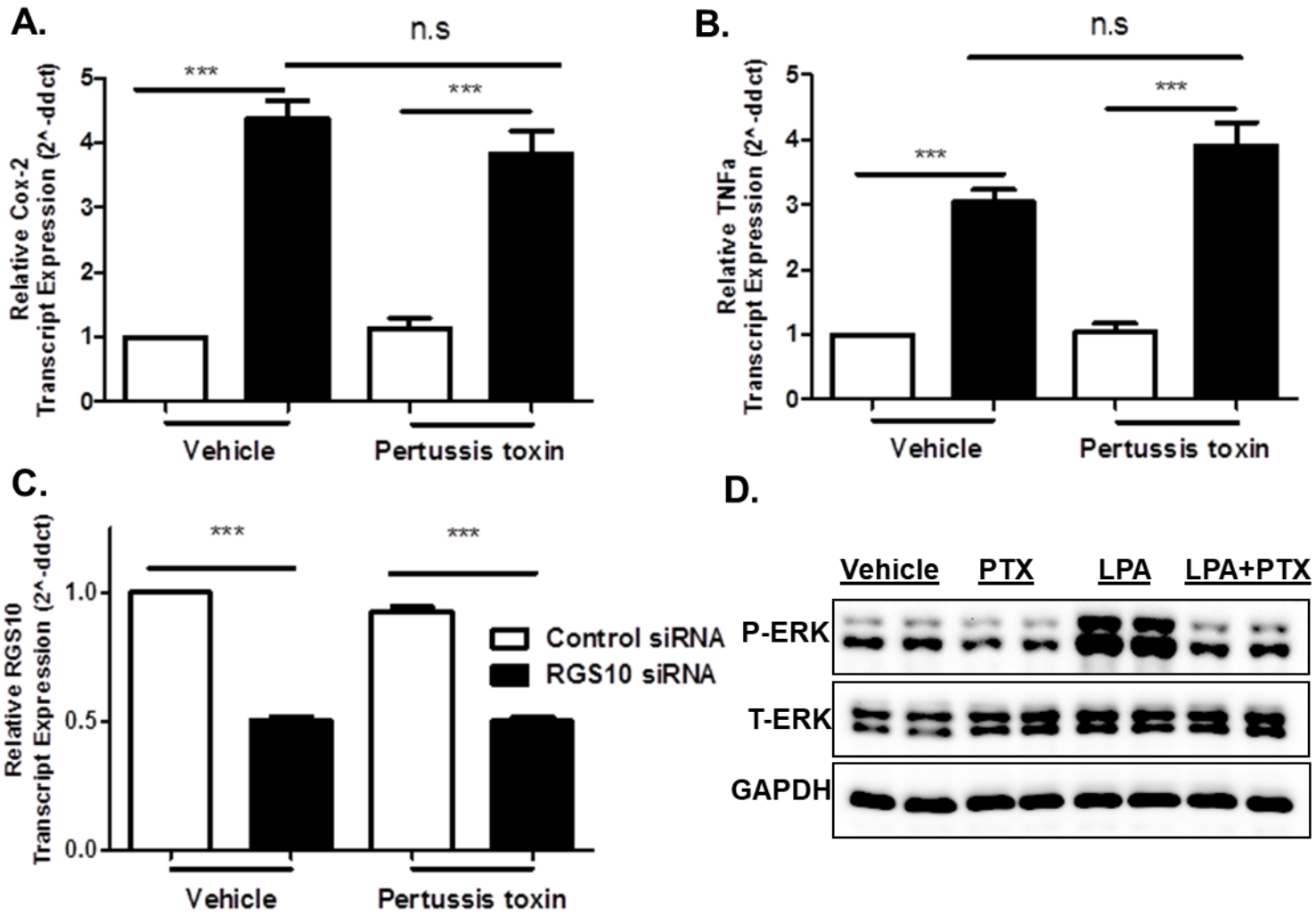

Figure 6